DIRECT NUMERICAL SIMULATION OF A SPATIALLY EVOLVING SUPERSONIC TRANSITIONAL/TURBULENT BOUNDARY LAYER

Hiroshi Maekawa
Graduate School of Engineering,
Hiroshima University
1-4-1 Kagamiyama, Higashi-Hiroshima-shi, 739-8527 Hiroshima, Japan
maekawa@mec.hiroshima-u.ac.jp

Daisuke Watanabe
Graduate School of Engineering,
Hiroshima University
1-4-1 Kagamiyama, Higashi-Hiroshima-shi, 739-8527 Hiroshima, Japan
watanabe@hiroshima-u.ac.jp

Kougen Ozaki
Graduate School of Engineering,
Hiroshima University
1-4-1 Kagamiyama, Higashi-Hiroshima-shi, 739-8527 Hiroshima, Japan
mkgnoz@hiroshima-u.ac.jp

Hajime Takami
Environmental Engineering Division,
Railway Technical Research Institute
2-8-38 Hikari-cho, Kokubunji-shi, 185-8540 Tokyo, Japan
takami@rtri.or.jp

ABSTRACT

Transition mechanism in supersonic flat plate boundary layers with isothermal walls up to $M = 3$ is studied using spatially developing DNS. The compressible Navier-Stokes equations are numerically solved using high-order upwind-biased compact schemes for spatial derivatives (see Deng, Maekawa, Shen,1996). Navier-Stokes characteristic boundary conditions are used in the streamwise and vertical directions, and periodic boundary conditions in the spanwise direction. Random disturbances of isotropic homogeneous turbulence with the intensity of 4% relative to the free-stream velocity are introduced at the inlet of a computational box for $M = 2.5$. The transition scenario consists of the following four stages: first, generation of staggered vortical structures upstream giving rise to streaks, which is rather oblique and sometimes bifurcated, secondly, elongation of streaks in the streamwise direction, thirdly, oscillation of streaks with a couple of oblique streamwise vortices and an incipient spot, and finally breakdown of the flow due to growth of the spot. The three latter phases in this scenario have been observed in the low-speed boundary layer experiments subjected to high levels of free-stream turbulence by Mastubara and Alfredsson (2001). The longitudinal growth of the streaks is closely related to transient growth theory. The distribution of the streamwise velocity fluctuation shows to be similar to the experimental result of the incompressible transitional boundary layer, when it is scaled by the displacement thickness and normalized with their respective maximum. At higher amplitude case of 5% for $M = 3$, staggered structures are also observed but spanwise large-scale spots with rather complicated vortical structures are generated downstream soon. The shape factor starts around 2.6 and decreases to a value of 1.42 in the turbulent region. Reynolds number based on the momentum thickness reaches 1400 in the turbulent region. The streamwise velocity fluctuations in the turbulent regime show a good agreement with the experimental result by Konrad (1993) for $M = 2.9$ turbulent boundary layers. Large-scale motions observed in the turbulent regions exhibit similarities to those that have been found in incompressible boundary layers. Turbulent statistics show that the spanwise scale of the large-scale structure is about 440 wall units, which is consistent with recent PIV measurements for the $M = 2$ turbulent boundary layer by Ganapathisubramani et al. (2006). As Adrian (2000) and others hypothesized that the large-scale coherence in the incompressible turbulent boundary layers is a result of individual hairpin vortices convecting as groups, the numerical results show that a few hairpin vortices generated on the lifted-up low-speed streak convect in the supersonic turbulent boundary layer. As stated for the turbulent spots in the transitional region, several hairpin vortices are generated all at once when the large spots grow and merge each other in the transitional boundary layer. This fact is consistent with the experimental observations of the large-scale coherence in the supersonic/incompressible turbulent boundary layers. In the simulation the skin friction coefficient for $M = 3$ is found to show a good agreement with experimental results for $2.2 < M < 2.8$ compiled by Coles (1954). The simula-

tion results for $M = 2.2$, 2.5 and 3 indicate that transition is delayed as Mach number increases due to the near wall density gradient.

INTRODUCTION

Over the last two decades, considerable progress has been made in studying incompressible boundary layer flows through experiments, theoretical analyses and quasi-periodic or spatial numerical simulations leading to a fairly comprehensive picture of the primary stage of transition scenarios and a characterization of structures of inhomogeneous turbulence and its properties. Numerical simulations have provided reliable databases necessary for the development of suitable turbulence models.

In contrast, the progress in the compressible regime has not been as large due to intrinsic difficulties both in the experiments and in the numerical simulations. The experimental measurements are limited to basic turbulence quantities and by the spatial resolution near the wall. The simulations have been hampered by low Reynolds number. The understanding of the primary stage of transition scenarios for supersonic boundary layers is even less pronounced due to the experimental and numerical difficulties. For transitional simulations, a spatial evolving simulation is essential. However, careful treatment of boundary conditions is required so that acoustic waves are not reflected back into the domain producing spurious results. Recently, a few direct numerical simulations of compressible turbulent boundary layers have been performed. Rai et al. and Gatski and Erlebacker performed a direct numerical simulation of a spatial evolving adiabatic flat plate boundary layer flow at supersonic Mach number ($M_\infty = 2.25$) that used a fourth-order accurate in space upwind-biased finite difference technique. More recently, Pirozzoli et al. simulated spatial evolving boundary layer at supersonic Mach number using weighted-ENO reconstruction of the characteristics inviscid fluxes. They introduced a region of blowing and suction to induce laminar-turbulent transition. The emphasis of their study is to assess the validity of *Morkovin's* hypothesis and Reynolds analogy, and the controlling mechanism for turbulence. The numerical results at Mach number of 2.25 show that the essential dynamics of the adiabatic turbulent boundary layer flow resembles closely the incompressible pattern.

In this study, a spatial DNS of a supersonic, isothermal flat plate boundary layer flow at $2.2 < M_\infty < 3$ is analyzed. Effects of both transition and boundary layer growth require the application of fully spatial formulation in a direct numerical simulation without appealing to either slow growth or extended temporal simplifying assumptions. The emphasis of this study is to assess the primary stage of transitional scenarios for supersonic boundary layer and the later stage of streak breakdown, and finally turbulent boundary layer for supersonic flow up to $M_\infty = 3$. Issues associated with the effects of freestream Mach number on the boundary layer flow with isothermal walls are addressed in this study, such as: (i) the streamwise vortices and streak formation; (ii) the streak breakdown and the turbulent spot; (iii) the turbulent spot amalgamation; (iv) the scaling laws of the turbulent boundary layer fluctuation statistics.

COMPUTATIONAL METHOD

To simulate and analyze in detail full configurations is not currently feasible, sufficient progress has been made to analyze the dynamics of simpler building block flows that provide useful insights into the underlying dynamics of full configuration compressible flows. One such flow is the spatially evolving flat plate supersonic boundary layer. In the present simulations, NSCBC (Navier Stokes characteristic boundary conditions) are used in the streamwise (x) and vertical (y) directions, whereas the periodic boundary conditions are employed in the spanwise (z) directions. A No-slip isothermal wall and non-reflecting boundary conditions are imposed at y=0 and upper far field. The length of the computational domain in the spanwise directions is determined from the previous turbulent boundary layer simulations (Guarini et al. 2001) and linear stability results. Linear stability analysis indicates that wall cooling stabilize the first-mode waves for $2.2 < M_\infty < 3$ (see Mack 1984), where no dominant second mode destabilized by cooling boundary layer. The three-dimensional first-modes are dominant in the supersonic boundary layer $2.2 < M_\infty < 3$. In the DNS of the spatially developing boundary layer, the nondimensional equations governing the conservation of mass, momentum, and energy for a compressible Newtonian fluid are solved. Note that displace thickness at the inlet boundary layer is chosen to the representative length scale. Therefore, as shown in Fig.1, the spanwise size is shown as $33\delta^*_{in}$, which is large enough for oblique disturbances. the Reynolds number based on the displacement thickness, the free stream velocity and wall viscosity is 1000 at the inlet. The free stream Mach number is ranging between 2.2 and 3. To obtain spatially accurate numerical solutions to the governing equations, high-order (fifth-order) upwind biased compact schemes (Deng, Maekawa & Shen, 1996) are employed to discretize the hyperbolic (Euler) terms, and sixth-order compact scheme (Lele, 1992) for the molecular terms. A forth-order Runge-Kutta scheme is used for time advancement. Computational details, such as flux splitting technique, grid stretching and minimum grid sizes in the x, y, z directions, are presented in Maekawa et al (2004).

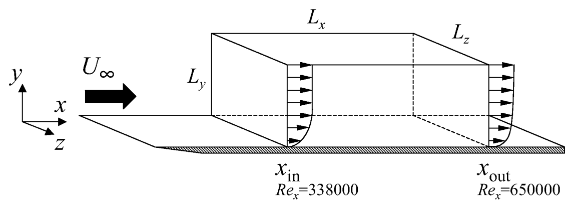

Figure 1: Sketch of the computational domain and Cartesian coordinates: Re_x indicates running Reynolds number based on the length from the plate inlet.

RESULTS

Streamwise Vortices and Streak Formation

The temporal approximation is only a crude approximation of a boundary layer spatially developing, where one works in a frame traveling with some velocity such as the group velocity or the averaged velocity in the boundary layer, in which the flow is homogeneous in the streamwise direction. We present DNS results of a spatial boundary layer, initiated upstream by a laminar velocity profile with a corresponding temperature profile superposed on the average flow, plus a random forcing generated with isotropic homogeneous compressible turbulence. Figure 2 shows top views of the boundary layer structures. The second invariant Q of the velocity gradient tensor is employed to represent the vortical structure and the surface plot of instantaneous streamwise velocities minus the laminar profile for the low-speed streak. Figure 3 shows successive snapshots of top view near the inlet. The oblique (not straight) Q structures are apparent first in the close-up view of (a), where low-speed streaks are observed on the periphery of Q structures. Further downstream, as seen in (b) and (c), due to the development of a pair of oblique Q structures, hairpin structures are generated above the lifted-up low-speed streak. These hairpin heads are successively created on the low-speed streak. As can be seen in the same figure, a packet of hairpins becomes a significant structure in the transitional boundary layer. The side view shows that the hairpin packet convects quickly due to the high-speed free stream velocity in the boundary layer.

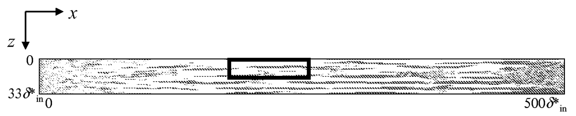

Figure 2: Streamwise vortices and streaks for $M = 2.5$ and $Re = 1000$: flow is forced with 4% disturbances. Window area corresponds to figure 3 (c).

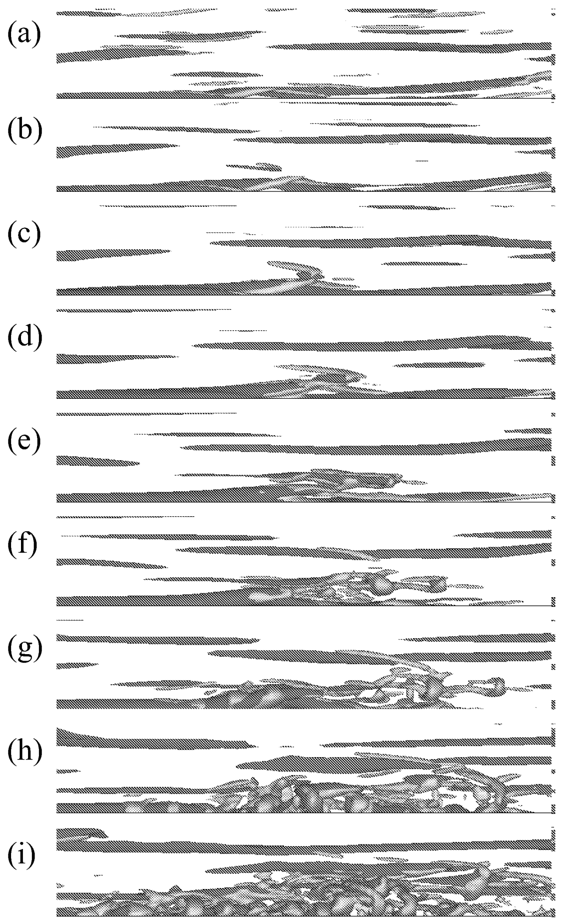

Figure 3: Downstream development of streamwise vortices and streaks: $u' = -0.1$ (dark gray) and $Q = 0.001$ (light gray).

Fourier Analysis of Velocity Fluctuation. Figure 4 shows the results of Fourier analysis for streamwise velocity fluctuations at various downstream locations, which may correspond to low or high-speed streaks near the wall. At $x = 66\delta^*_{in}$, a fluctuation peak is observed at wave number β of 1.8 and at about displacement thickness height. The wavenumber of 1.8 corresponds to the width of the spanwise direction, such as $2\pi/\beta \times \delta^*_{in}$ in the simulation. This fact indicates that the spanwise scale of the streaks approaches the boundary layer thickness, which shows a good agreement with the experiments in the incompressible boundary layer subjected to free stream turbulence. Further downstream locations at $x = 380\delta^*_{in}$, a peak is seen at wave number of $1.1 \sim 1.3$ which is the same as or somewhat less than the observation at $x = 66\delta^*_{in}$, because boundary displacement thickness at $x = 380\delta^*_{in}$ is 1.5 times large as that at $x = 66\delta^*_{in}$. Note that turbulent spots are developing at $x = 380\delta^*_{in}$

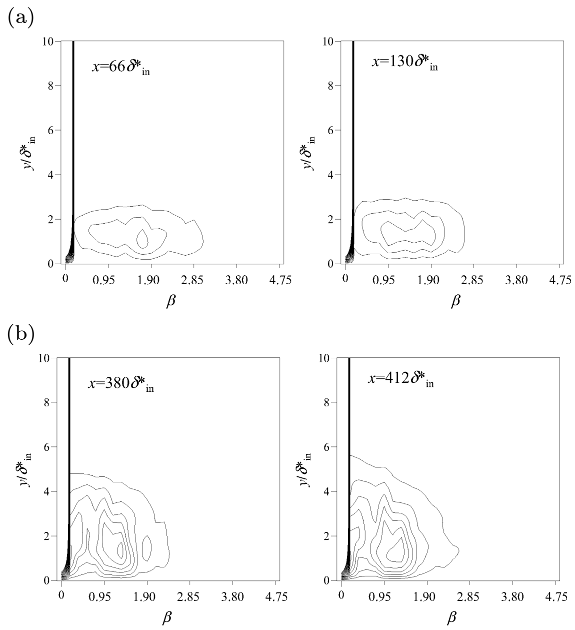

Figure 4: Wavenumber spectra at different downstream locations for $M = 2.5$ and $Re = 1000$: flow is forced with 4% disturbances.

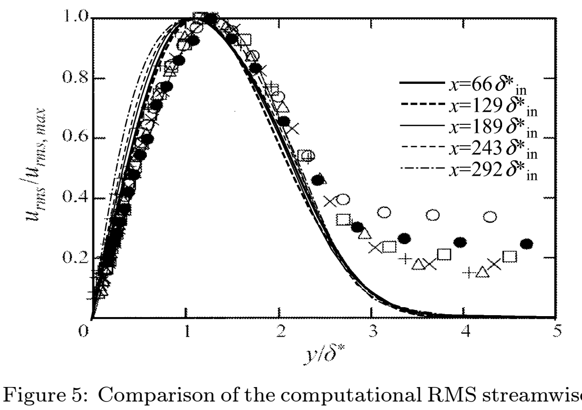

Figure 5: Comparison of the computational RMS streamwise velocity profile with experimental data (symbols) of Matsubara and Alfredsson (2001).

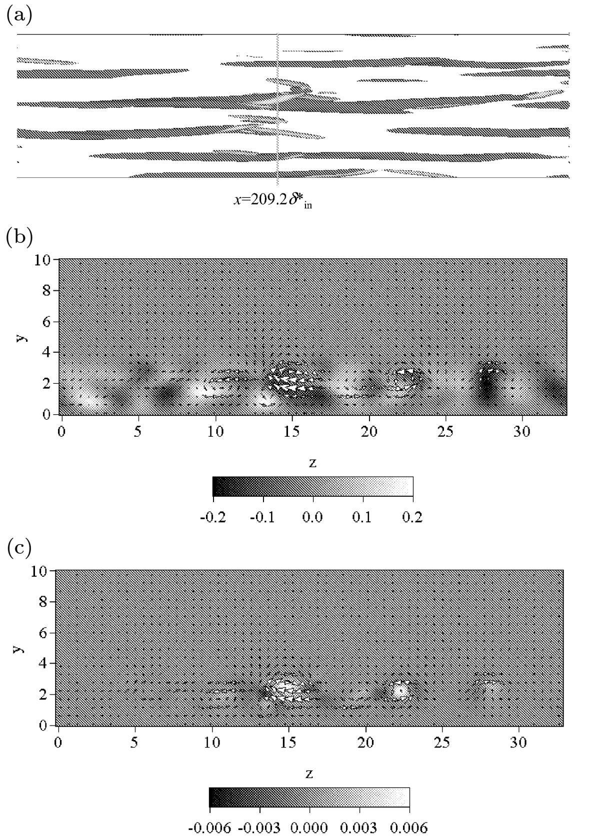

Figure 6: Beginning of turbulent spot due to a pair of oblique vortices at the same normal location: (a) Top view of streamwise vortices and streaks; (b) Low- (minus) and high-speed (plus) streaks and velocity vector in the y-z plane at the location shown in (a); (c) Q structures (plus), strain dominant structure (minus) and velocity vector in the y-z plane shown at the location shown in (a).

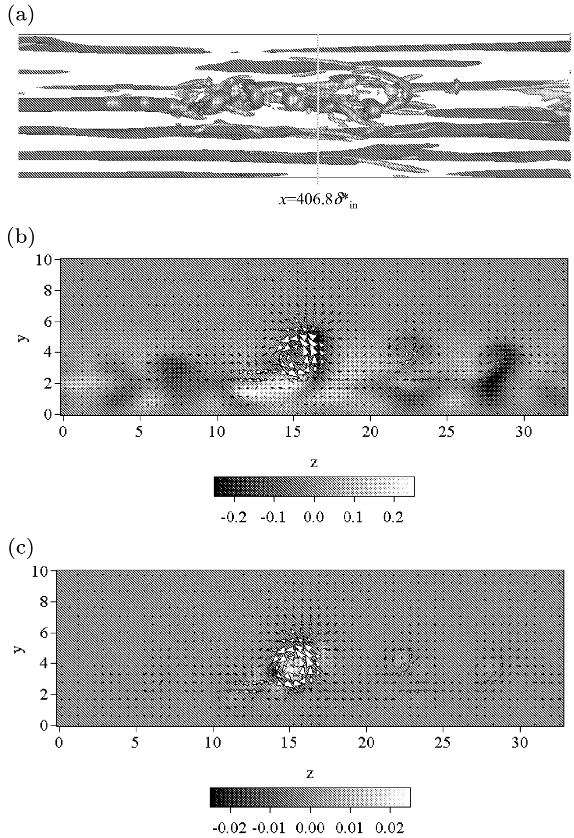

Figure 7: Structure of turbulent spot: $Q = 0.001$ and $u' = -0.1$: (a) Top view of streamwise vortices and streaks; (b) Low- (minus) and high-speed (plus)streaks and velocity vector in the y-z plane at the location shown in (a); (c) Q structures (plus), strain dominant structure (minus) and velocity vector in the y-z plane at the location shown in (a).

Streamwise Velocity Fluctuation. Streamwise velocity fluctuations are measured at various downstream locations. Figure 5 shows the distribution of streamwise velocity fluctuation scaled by the local displacement thickness and normalized with their respective maximum. Figure 5 also presents the experimental results of the transitional incompressible boundary layer measured by Matsubara and Alfredssson, (2001). The numerical profiles are similar to the experimental data, but not self-similar as the experimental profiles. The most profile peak locations slightly move to the wall compared to the experimental results. Scaling by the local displacement thickness would be modified for supersonic boundary layers.

Turbulent Spot

As shown in figures 3 (c),(d),(e) and (f) and figure 6, the primary low-speed streak deforms due to the development of hairpin vortices and the secondary streak appears near by the primary one. The lifted-up primary streak with hairpin packets leads to strongly retarded streamwise momentum. Therefore, this configuration leads to streak breakdown, as shown in figure 7. This fact indicates that the local velocity profile plays an important role to make a turbulent spot. The large-scale motion observed in a turbulent spot originates partly from the streak configuration with hairpin vortices developing in the streamwise direction.

Successive snap shots indicate that hairpin packets observed downstream are developing in the streamwise direction first. Then a cluster of hairpin packets grows in the spanwise direction. As can be seen in the top views of the incompressible boundary layer flow visualization, structures develops less dependently on the other packet structure first leading to the large-scale structure in the streamwise x, vertical y and spanwise z directions. This mechanism leads to the inclined hierarchic structure in turbulent spots in the supersonic boundary, hairpin packets in the outer region and inner mushroom-like density visualized structures which is still similar to the experimental observations in high Reynolds number turbulent boundary layers (see Matsubara and Alfredsson 2001). In the experiment of a supersonic turbulent boundary layer by Ganapathisubramani et al. (2006), two point correlations show large-scale structures increasing trend in the streamwise length scale with normal location. The spanwise scale of the uniform-velocity strips increases with increasing wall-normal distance. The essential features found in the turbulent spots and the marginal process with each other are very close to the experimental finding of the supersonic boundary layer.

Downstream Turbulence Statistics

Mean Flow Evolution. For $M = 3$, the flow is forced with 5% intensity disturbances. Turbulent spots are developing, merging each other downstream, and the turbulent boundary layer are observed in figure 8. Figures 9 (a) and (b) show evolutions of the shape factor of the mean velocity profile and the boundary layer displacement thickness, respectively. This figure indicates that transition is delayed as Mach number increases with the same level of inlet random disturbances. A comparison of the numerical result for $M = 2.5$ with the disturbance intensity of 4% (shown in dashed line) and 4.5% (dotted line) shows that there is a threshold value to induce transition to turbulence. Furthermore, a comparison of the numerical results for $M = 2.2$ (solid line) and those for $M = 2.5$ (dashed line) with the same disturbance intensity of 4% indicates that transition is delayed as Mach number increases.

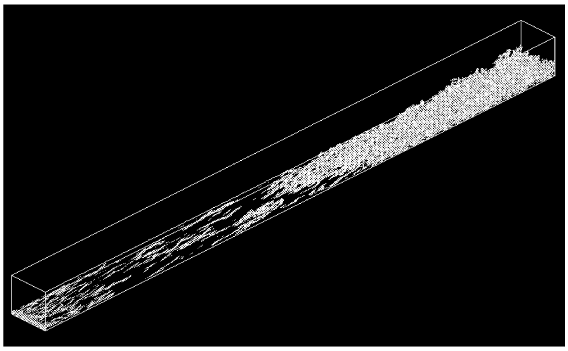

Figure 8: Bird-eye view of boundary layer for $M = 3$: flow is forced with 5% disturbances; Q is used to visualize the transitional/turbulent flow.

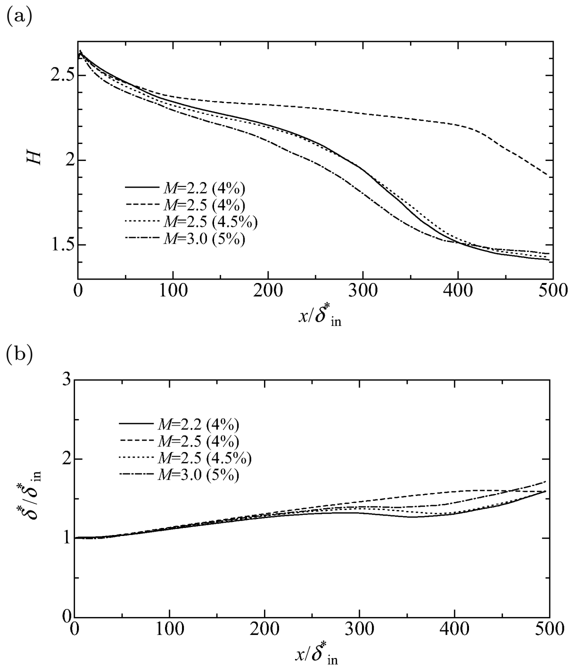

Figure 9: Evolution of mean velocity profile:(a) Shape factor;(b) Boundary layer displacement thickness.

The skin friction coefficient is defined as

$$C_f = 2\left(\frac{u_\tau}{U_\infty}\right)^2 \frac{\bar{\rho}_w}{\bar{\rho}_\infty}. \qquad (1)$$

Figure 10 depicts the skin friction coefficient for $M = 2.5$ and 3.0 flows as a function of the Reynolds number based on the boundary layer momentum thickness. Also included in figure 10 are the experimental data of Coles (1954) and the skin friction correlation given in Bardina (1997), as well as the laminar flow skin friction coefficient for an isothermal wall condition. There are very few experimental studies at the low Reynolds number of the simulation. However, the turbulent simulations compare favorably with the experimental results.

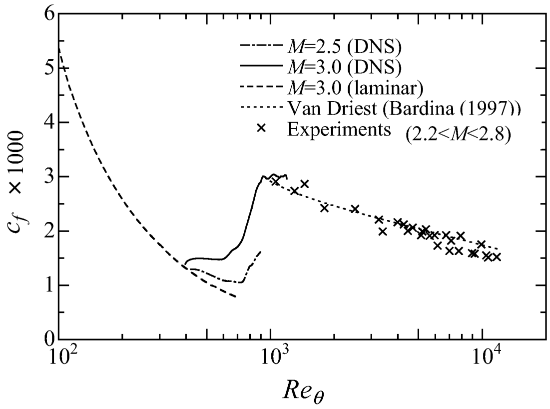

Figure 10: Comparison of the computational skin friction coefficient with experimental data of Coles (1954).

RMS Velocity. Figure 11 shows RMS data of the streamwise velocity fluctuation for $M = 3$ at a downstream location with the experimental results measured by Konrad (1993) for the $M = 2.9$ turbulent boundary layer. He used a normal hot-wire close to the wall instead of crossed wire probes, where the effect of low Mach number is serious for crossed wires. Therefore, in the experiments good collapse is obtained for the streamwise component but the experiments are inconclusive with respect to the collapse of the other components. There is an additional point which need to be mentioned in connection with figure 11. Unlike adiabatic wall boundary layers, Reynolds number based on local viscosity in the boundary layer simulation with an isothermal wall does not vary much across the boundary layer (less than 25% increase). The experimental Reynolds number of the turbulent boundary layer with an adiabatic wall is much higher than the simulation result, so that the viscosity effect on the velocity measurement for the probe point near the wall shown in figure 11 may be not so serious as the low Reynolds number experiment.

CONCLUSIONS

Results from three-dimensional spatial direct numerical simulations of an isothermal supersonic boundary layer provide new physical insights into three-dimensional evolutions of the streamwise vortices and the streak, the turbulent spot, and the characteristic features of the supersonic turbulent boundary layer. Forcing with isotropic homogeneous turbulence at the laminar inlet flow yields large-scale motions that increase in the streamwise length scale with normal loca-

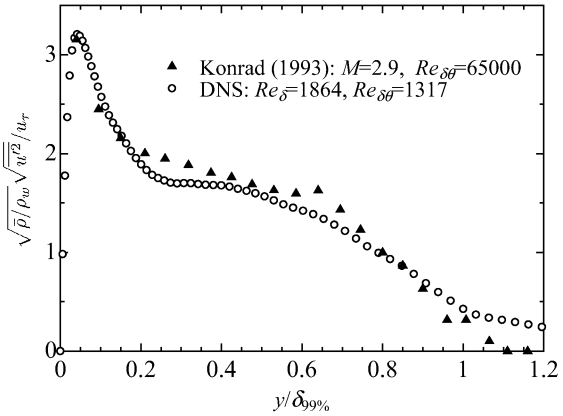

Figure 11: Comparison of the computational RMS streamwise velocity profile with experimental data of Konrad (1993).

tion in the transitional and turbulent boundary layer. This feature largely originates from the transitional structure of streak breakdown, in which hairpin packets and lifted-up low speed streak play an important role. A comparison of the numerical results for different Mach numbers indicates that transition is delayed as Mach number increases mainly due to the near wall density gradient. The numerical statistical results, such as the skin friction coefficient and RMS velocity, show a good agreement with the experiments.

REFERENCES

Adrian, R.J., Meinhart, C.D., and Tomkins, C.D., 2000, "Vortex organization in the outer region of the turbulent boundary layer", Journal of Fluid Mechanics, Vol.422, pp.1-53.

Bardina, J.E., Huang, P.G., and Coakley, T.J., 1980, "Turbulence modeling validation, testing, and development", NASA Tech. Memo. No. 110446.

Coles, D., "Measurements of turbulent friction on a smooth flat plate in supersonic flow", J. Aero. Sci., Vo.21, pp.433-448.

Deng, X., Maekawa, H., and Shen, C., 1996, " A Class of High Order Dissipative Compact Schemes", AIAA Paper, No. 96-1972, pp 1-11, New Orleans, LA.

Ganapathisubranmani, B., Clements, N.T., and Dolling, D.S., 2006, " Large-scale motions in a supersonic turbulent boundary layer", Journal of Fluid Mechanics, Vol.556, pp.271-282.

Gatski, T.B. and Erlebacker, G., 2002, "Numerical simulation of a spatially evolving supersonic turbulent boundary layer", NASA Tech. Memo. No.211934.

Guarini, S.E., Moser, R.D., Shariff, K., and Wray, A., 2000, "Direct numerical simulation of a supersonic turbulent boundary layer at Mach 2.5", Journal of Fluid Mechanics, Vol.414, pp.1-34.

Konrad, W., 1993, "A three-dimensional supersonic turbulent boundary layer generated by an isentropic compression", PH.D. Thesis, Princeton University, Princeton, NJ.

Lele, S. K., 1992, " Compact finite difference schemes with spectral-like resolution", *J. Comput. Phys.*, **103**, pp.16-42.

Mach, L.M., 1984, "Boundary-layer linear stability theory", AGARD Rept. 709pp. 3.1-3.81.

Maeder, T., Adams, N.A., and Kleiser, L., 2001, "Direct numerical simulation of supersonic boundary layers by an extended temporal approach", Journal of Fluid Mechanics, Vol.429, pp.187-34.

Maekawa, H., Watanabe, D. and Yamashita, K., 2004, "DNS of supersonic transitional and turbulent flows", Proc. of International Workshop on Advances Computational Method, Tokyo.

Matsubara, M. and Alfredsson, P.H., 2001, " Disturbance growth in boundary layers subjected to free stream turbulence", Journal of Fluid Mechanics, Vol.430, pp.149-168.

Pirozzoli, P., Grasso, F. and Gatski, T.B., 2004, "Direct numerical simulation and analysis of a spatially evolving supersonic turbulent boundary layer at M=2.25", Physics of Fluids, Vol. 16, No.4, pp.530-545.

Poinsot, T.J. and Lele, S.K., 1992, " Boundary conditions for direct simulations of compressible viscous flows", J. Comput. Phys. Vol. 101, pp.104-129.